# DEVELOPMENT OF MULTI-ZONE CHEMISTRY MAPPING FOR TURBULENT PARTIALLY PREMIXED CMBUSTION

**M. Jangi, R. Yu and X. S. Bai**
Mehdi.jangi@energy.lth.se
Div. of Fluid Mechanics, Dept. of Energy Sciences, Lund University, P.O. Box 118, S 221 00 Lund, Sweden

## Abstract
A direct numerical simulation (DNS) coupling with multi-zone chemistry mapping (MZCM) is presented to simulate flame propagation and auto-ignition in premixed and partially premixed fuel/air mixtures. In the MZCM approach, the physical domain is mapped into a low dimensional phase space with a few thermodynamic variables as the independent variables. The integration of the chemical reaction rates and heat release rate are done on the grids in the phase space. It is shown that for premixed mixtures, two independent variables can be sufficient to construct the phase space to achieve a satisfactory mapping. The two variables can be temperature of the mixture and specific element mass ratio of H atom for fuels containing hydrogen atom. However, for partially premixed mixtures where combustion may be in both premixed and non-premixed flame modes, a third phase space variable is required to map the physical cell into the phase-space. It is shown that scalar dissipation rate of the element mass ratio of H atom can be used as the third dimension of the phase space. An investigation is carried out on the behavior of MZCM and the choice over the element on which the local element mass ratio should be based on. An aliasing error in the MZCM is investigated. It is shown that if the element mass ratio is based on the element involved in the most diffusive molecules, the aliasing error of the model can approach to zero when the grid in the phase space is refined. To validate the MZCM model the results of DNS coupled with MZCM (DNS-MZCM) are compared with full DNS that integrates the chemical reaction rates and heat release rate directly in physical space. Good agreement between the results from DNS and DNS-MZCM is obtained while the computational time is reduced at least 70%.

## Introduction
Combustion may be classified into different categories; e.g. premixed and non-premixed flames or a mix of both. It has been shown that many premixed and non-premixed flames are actually stratified or partially premixed flames. The Sandia jet-flames, Flame-D – Flame-F [1], for example, may be considered as a non-premixed jet flames however, it has been shown that none of the conventional premixed/non-premixed approaches can properly describe the behavior of the flames observed in the experiments [2]. Generally speaking, the conventional premixed/non-premixed approaches are not able to describe a turbulent reacting flow, if the scale of reaction zone is of the order of the smallest flow motions, e.g. Kolmogorov scales in turbulent combustion. At these conditions, flow motions and diffusion of the heat and mass to/from preheat and post-flame zone constantly change the temperature and concentration of the species at the reaction front. This means that, neither of the assumption of a perfectly mixed reactants before reaching to the reaction zone, nor perfectly non-premixed fuel and oxidizer mixing that limits the reaction to be in a very thin layer where the mixture is at the stoichiometric, is valid. One may define a partially premixed combustion as a reacting flow in which the fuel-rich and fuel-lean regions coexist in the domain, as such there are lean and rich premixed flames and diffusion flames found in the domain [3]. Different from partially premixed flames, stratified premixed flames are essentially premixed flames with varying equivalence ratio in the domain.

To properly describe the chemical reactions, diffusion and turbulent mixing processes in the domain, a usage of computational cell resolution of the order of one hundredth to one tenth of the reaction zone is required. The current computational powers, however, are limited to provide such resolution only for small and simple geometries, e.g., a cube with 5 mm in length, and simple fuels, e.g. hydrogen or methane [4]. Computational costs of such a directly resolved chemistry-flow in spatial grids are tremendously high especially if detailed chemistry is taken to account. Therefore, it is necessary to develop methods and models that are computationally affordable. These types of methods allow us to deal with the problem with partially premixed nature such as those of Sandia flames D-F, extinction and re-ignition of triple flames and combustion in PPC type engines.

In a turbulent combustion, since the ODEs of chemical kinetic mechanism is usually very stiff, resolving chemical time in a CFD time step is the heaviest part of the computation. Mapping kinetic mechanism to a lower dimensional thermodynamic space is a tool that allows computing turbulent combustion to include detailed chemistry. Computational singularity perturbation (CSP) approach by Lam et al. [5], and the intrinsic low-dimension manifold (ILDM) approach by Maas and Pope [6] are of this type. The classical methods to map thermodynamic state to a low dimensional manifold are based on identification of those species that are in the equilibrium within a flow time scale and eliminate them from the kinetic mechanism.

Multi-zone chemistry mapping is another approach. In our previous study, we developed a method for mapping a premixed combustion to a two dimensional thermodynamic state based on multi-zone chemistry mapping (MZCM) [7]. Multi-zone approach was developed first in late 1990s for modelling NOx formation in homogeneous charge compression ignition (HCCI) engines [8]. The main idea behind the CFD multi-zone chemistry mapping approaches is to integrate the chemical reaction rates in low-dimension chemistry zones. Each zone corresponds to a number of different CFD cells in the physical domain, thereby integration of the chemical reaction rates and heat release is not performed in every cell in the physical domain. The results in the chemistry zones are subsequently integrated to the flow transport terms in every cell in the physical domain. This procedure decreases the computational cost significantly since it is possible to group the physical cells into much smaller number of zero-dimensional chemistry zones. The key issue of multi-zone approach is the mapping between the physical domain and the multi-zone domain.

The goal of this work is to extend and validate our previous MZCM approach to simulate a partially premixed flame. MZCM is coupled with DNS of the flow transport (hereafter referred to as DNS-MZCM) to simulate ignition and flame propagation in premixed and partially premixed fuel/air mixtures. The results are compared with the results of DNS in which the integration of the chemical reaction rates and heat release is directly carried out in the CFD cells in the physical domain. DNS approach is employed here to eliminate extra modelling uncertainties in RANS and LES to allow for an adequate evaluation of the MZCM approach. The DNS data offer a possibility of comparing not only the global properties such as pressure and mean flame growth, but also the detailed reaction zone structures and finite-rate chemistry related phenomena.

## Model description and numerical methods

Ignition and flame propagation in premixed and partially premixed fuel/air mixtures under various flow and mixture conditions in a constant volume enclosure are considered. The flow is assumed to have low Mach numbers. The mean initial flow velocity is assumed to be zero in the enclosures. The mean initial turbulence field is generated by superimposing a set of synthesized Fourier waves [9] to the mean flow field such that the waves satisfy the energy spectrum suggested by Pope [10]. Fuel in this study is a mixture of $H_2$/CO/$N_2$ known as

Syngas. The kinetic mechanism given in ref. [11] is used. This mechanism involves 13 species and 35 elementary reactions. In Cartesian coordinates $x_i (i = 1,2,3)$ and under the low Mach number assumption, the acoustic effect is neglected. The pressure is decomposed to two parts, the hydrodynamic pressure that drives the flow and the thermodynamic pressure that is uniform in the entire flow field. The governing equations for such reacting flow field are made up of the continuity equation, the momentum equations; the species transport equations, and the energy equation. The species transport equations can be written as follows,

$$\frac{\partial \rho Y_k}{\partial t} + \frac{\partial \rho u_j Y_k}{\partial x_j} = \frac{\partial}{\partial x_j}\left(-\rho Y_k V_{k,j}\right) + \dot{\omega}_k \qquad (K = 1...N), \tag{1}$$

where ρ is the density of mixture; $t$ is time; $u_j$ is the component of velocity vector in $x_j$ direction; $Y_k$ is the mass fraction of $k$-th species. $V_{k,j}$ is the component of diffusion velocity of $k$-th species in $x_j$ direction; $\dot{\omega}_k$ is the reaction rate of $k$-th species and $N$ is the total number of species in mixture. The conservation of energy yields the following equation:

$$\rho C_p \frac{DT}{Dt} = \frac{DP}{Dt} + \frac{\partial}{\partial x_i}\left(\lambda \frac{\partial T}{\partial x_i}\right) - \rho \frac{\partial T}{\partial x_i} \sum C_{p,k} Y_k V_{k,i} - \sum h_k \dot{\omega}_k, \tag{2}$$

where $T$ is temperature; $P$ is the thermodynamic pressure; $\lambda$ is thermal conductivity; $C_p$ is the specific heat at constant pressure; and $h_k$ is the specific enthalpy of the $k$-th species.

The equation of state is used to provide an additional relation among the thermodynamic pressure, temperature, density and the species mass fractions. The reaction rates are calculated using Arrhenius expressions based on corresponding chemical kinetic mechanisms. Detailed transport is considered to determine the mass diffusion velocity.

The governing equations are numerically solved using a high order finite difference method on uniform Cartesian grids. The numerical solver is based on the fractional step method similar to the method of Day and Bell [12]. The diffusion terms and pressure gradients in the governing equations are descritized using 6th order central scheme. For the convective terms 6th order central difference scheme and alternatively 5th order WENO scheme [13] is used depending on the smoothness of the dependent variables. No explicit spatial filtering of the numerical solution is needed owing to the use of the non-oscillatory schemes. The discretized system for the flow transport Eq.(4) is integrated in time using a third order Runge-Kutta scheme [14]. Temporal integration of the flow transport is performed using an adjustable time step with CFL < 0.1. The solver is parallelized based on domain decomposition [15].

To eliminate the stiffness in the equations and to resolve the chemical time, a chemistry solver similar to the constant pressure module of SENKIN [16] is used to integrate the chemistry fractional step Eq. (3) for an interval started from $t=t_n$ and ended at $t_{n+1}=t_n+\Delta t$ . The initial field of the chemical integration step, e.g. the mass fractions, temperature and thermodynamic pressure in the computational cells is specified at time $t=t_n$ and the pressure is constant during this fractional step. One may perform the integration of the chemistry step Eq. (3) for all cells of the physical domain and during each time step $\Delta t$. This is the full DNS approach with which the computational cost rapidly increases as the number of cells in the physical domain increases. A more efficient way of integrating the chemistry step is the MZCM approach discussed below.

**Multi-zone chemistry mapping (MZCM)**

The basic idea behind the MZCM approach is that in a reactive flow field involving flame propagation and auto-ignition, there are computational cells in which the composition and

temperature at time step $t=t_n$ differ very little so that the integration of the chemistry fractional step Eq. (3) gives the same result, regardless the local flow convection and diffusion, since the chemical reaction rates are functions of the species concentration, temperature and pressure only. The integration can be done once for all these similar cells; in this way the computational cost can be greatly reduced.

Two technical questions arise; (a) how to group and map the thermodynamic state similar cells in the physical domain into one zone, and (b) how to make sure the resulting error in the grouping and mapping procedure is low. Different mapping methods have been developed in the literature, however, the error introduced in the mapping procedure has not been thoroughly analysed. To describe the MZCM procedure, rewrite the chemistry fractional step Eq. (3) into the following equivalent form,

$$\frac{d(\rho Y_k)}{dt} = \dot{\omega}_k, \qquad (t_n < t \le t_n + \Delta t, k = 1 \quad \dots \quad N), \tag{3}$$

With initial condition,

$$(Y_k, T, P) = (Y_k, T, P)^n, \qquad (t = t_n, k = 1 \quad \dots \quad N). \tag{4}$$

Note that density is determined from the mass fractions, thermodynamic pressure and temperature through the equation of state.

For idealized homogeneous mixtures that have the same concentrations of constituents and the same temperature in the field, all cells in the physical domain undergo the same chemical reactions. The cells can be mapped to one zone. The state of the zone may be characterized using temperature as an indicator for the reaction progress. HCCI combustion is close to the above-discussed idealized reactor with homogeneous mixture; however, in practice the temperature field is not homogeneous due to wall heat transfer. In such case, the cells in the physical domain can be mapped to different zones according to the initial temperature in the cells. The reaction progress in different zones is different. If the chemical reactions are much faster than the flow transport, e.g., the ignition process is completed within one flow time step, then mixing between different cells in the physical domain may be neglected. The integration of the chemistry fractional step Eq. (5) depends only on the initial temperature field and initial thermodynamic pressure, since the mass fractions of species in the physical domain is homogeneous. Since the thermodynamic pressure in low Mach number flows is homogeneous in the physical domain, the MZCM can be conveniently done based on the initial temperature field only. Earlier multi-zone modelling of HCCI combustion based on temperature zones [8] showed promising results.

Extension of the multi-zone modelling can be done to mixtures with stratifications in both temperature and concentration. If the flow transport between the physical cells is negligible, the initial field required in Eq. (6) can be fully determined using temperature and mixture fraction (or alternatively local equivalence ratio) [17].

In reality, the mixing of species and heat transfer due to flow transport between the physical cells cannot be neglected. Typical example is the local laminar flame propagation where both the reactions and molecular diffusion are important. The initial condition at an intermediate CFD time step $t=t_n$ in Eq. (6) cannot be determined from the initial un-reacted mixtures. A most accurate but expensive way is to compare the entire species mass fractions and temperature $T$, $Y_k$ in the physical cells and group those cells that have similar $T$, $Y_k$. This is to map the three dimensional physical domain to a $N+1$ dimensional space, where $N$ is the total number of species in the flow field.

A more efficient way is mapping the physical domain into a low dimensional phase space. In the following we present a mapping approach for premixed mixtures based on two scalars, temperature and the specific element mass ratio of H atom. We shall then extend this mapping

approach to the partially premixed cases via introducing a third dimension to the phase space. This third dimension is an indicator of the mixing processes in the physical cells.

First, the mass fraction of an element *E,* $Y_k$, is determined from the species mass fractions in the mixture,

$$Y_E = \sum \frac{W_E}{W_k} \alpha_{E,k} Y_k. \tag{5}$$

where $W_E$ and $W_K$ are the atomic/molecular weights of the element $E$ and the $k$-th species respectively. $\alpha_{E,k}$ is the number of atoms of type $E$ in the $k$-th species.

The specific element mass ratio $Z_E$ can be written as

$$Z_E = \frac{Y_E}{Y_{E,st}}, \tag{6}$$

where subscript *st* denotes the stoichiometric mixture.

Next step is to compute the specific element mass ratio of atom $E$ in every cell in the physical domain; then the cells in the physical domain are mapped to the $T$-$Z_E$ space. Let a phase space be defined by $N_T$ number of temperature zone and $N_T$ number of $Z_E$ zones. For uniform zones in the phase space, the intervals of temperature $\Delta T$ and the specific element mass ratio $\Delta Z_E$ are

$$\Delta T = \frac{T_{max} - T_{min}}{N_T}, \quad and \quad \Delta Z_E = \frac{Z_{E_{max}} - Z_{E_{min}}}{N_Z}. \tag{7}$$

In the above equations, $T_{max}$ and $T_{min}$ are the maximum and minimum temperatures found in the physical cells at $t_n$. $Z_{E_{max}}$ and $Z_{E_{min}}$ are the maximum and minimum of $Z_E$ that are found in the physical cells at $t_n$. In discretized form the mapping is between the indexes $(i,j,k)$ of the cells in the physical domain to the index $(m,l)$ of the zones in the phase space. For each cell in the physical domain, cell indices, i.e., $i_{T(i,j,k,t_n)}$ and $i_{Z(i,j,k,t_n)}$, in the phase space are stored, which will be used later for the procedure of mapping back the multi-zone results. The $(i,j,k)$ cell in the physical domain is uniquely mapped to $(m,l)$ zone in the phase space according to,

$$\begin{aligned} i_T(i,j,k,t_n) &= m, \quad if \quad T(m) < T(i,j,k,t_n) \le T(m) + \Delta T \\ i_Z(i,j,k,t_n) &= l, \quad if \quad Z_E(l) < Z_E(i,j,k,t_n) \le Z_E(l) + \Delta Z_E. \end{aligned} \tag{8}$$

Each of the zones in the phase space may correspond to multiple cells in the physical domain. The mean values of the variables in the phase space zones, $Y_{MZ,k}(m,l,t_n)$, $T_{MZ}(m,l,t_n)$ and $P_{MZ}(m,l,t_n)$ are determined and used as the initial condition for the chemistry fractional step. The mean values of $Y_k$ in the phase space zones is calculated as the following

$$Y_{MZ,k}(m,l,t_n) = \frac{1}{N_{PC}} \sum \{Y_k(i,j,k,t_n) \mid i_T(i,j,k,t_n) = m, i_Z(i,j,k,t_n) = l\}, \tag{9}$$

where $N_{PC}$ is the number of physical cells that fall into the $(m,l)$ zone in the phase space.

Similarly, the mean $T$ in the phase space zones is calculated. Once the initial condition is determined for all zones in the phase space, integration of the chemistry fractional step is performed to obtain $Y_{MZ,k}(m,l,t_n)$ and $T_{MZ}(m,l,t_n)$. Then, the results are mapped back to the cells in the physical cells using the stored mapping index, i.e.,

$$\begin{aligned} Y_k^*(i,j,k,t_n + \Delta t) &= Y_{MZ,k}(i_T(i,j,k,t_n),(i_T(i,j,k,t_n),t_n + \Delta t) \\ T^*(i,j,k,t_n + \Delta t) &= T_{MZ,k}(i_T(i,j,k,t_n),(i_T(i,j,k,t_n),t_n + \Delta t), \end{aligned} \tag{10}$$

Density is then determined from the equation of state. Finally, the integration of the flow transport fractional step is performed to calculate the dependent variables at $t_n + \Delta t$ .

The thermodynamic pressure at $t_{n+1}$ is determined from global mass conservation in the constant volume enclosure according to the following relation:

$$P^{n+1} = M / \int (R_u \Sigma \frac{Y_k^{n+1}}{W_k} T^{n+1})^{-1} dV, \tag{11}$$

where $M$ and $V$ are the mass and volume of the computational domain, respectively, $R_u$ is the universal gas constant, and $W_k$ is the molecular weight of species $k$. In the present constant volume enclosure $M$ and $V$ are constant ($M$ determined from the initial condition and $V$). Fig. 1 shows the flowchart of the DNS-MZCM procedure in one CFD time step.

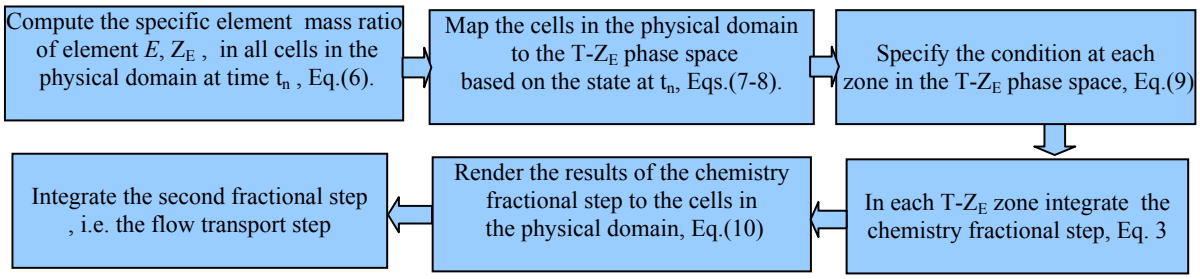


**Figure 1**. Flowchart of the DNS-MZCM procedure.

## MZCM approach for premixed combustion

To evaluate the multi-zone chemistry mapping approach we start with a test case where a premixed flame propagates in an initially homogeneous turbulence field of a stoichiometric H2/CO/N2-air mixture. The compositions of H2, CO and N2 are respectively 21%, 24%, and 55% on volume basis. The initial pressure and temperature of the domain are set to 0.5 MPa and 290 K, respectively. This test case is given in Table 1 as PC (premixed combustion).

**Table 1.** Initial conditions and computational domain.

| case | H2/CO/N2 | *T, K* | *P, MPa* | $Re_l$ | $\Delta X, \mu m$ |
|---|---|---|---|---|---|
| PC | 24:21:55 %vol. | 290 | 0.5 | 390 | 10 |
| PPC | 50:50:00 %vol. | 1100 | 0.5 | 150 | 10 |

Numerical simulation using the fractional step method described above is performed. The computation is carried out in a two dimensional domain with a dimension of 5mm×5mm using 512×512 computational cells. Periodic boundary conditions are used on all boundary faces. The flames were initiated by imposing a high initial temperature zone of the thickness of 0.175 mm at 2 mm from the left side of the enclosure. The initial temperature in the hot zone was set to 2200 K while the initial composition of the mixture in the hot zone is the same as that in the rest of the domain. Auto-ignition of the mixture in the hot zone starts first; then the two premixed flames propagate to the unburned mixtures. Figure 2 shows schematic of the computational domain and initial conditions for the test case.

Based on the kinetic mechanism used for this study the species in this reactive system are H2, O2, CO, H, O, OH, H2O, HO2, H2O2, HCO, CO2 and N2. Four elements are involved in the system, i.e. hydrogen, oxygen, carbon and nitrogen atoms. In the kinetic mechanism N2 is assumed to be inert gas. Therefore there are three options to define element mass fractions base on H, O or C, i.e., $Y_H$, $Y_O$ or $Y_C$.

Shown in Figure 3 are snapshots of temperature and $Z_H$ in the physical domain, and the scatter plot of physical cells in the $T$-$Z_E$ space at the same instance of time. The results are from full DNS with the kinetic mechanism involving 13 species and 35 reactions [11].

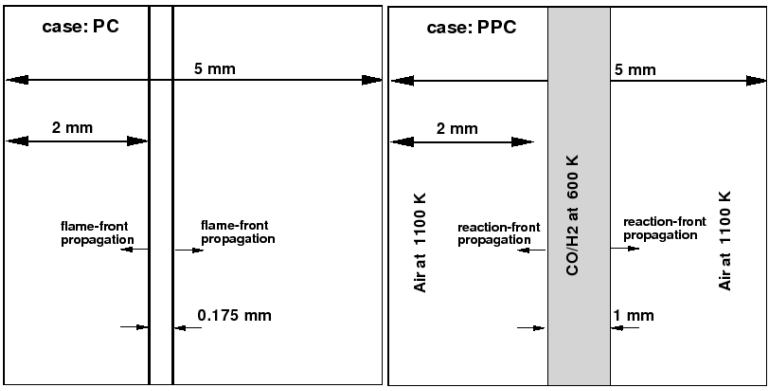


**Figure 2**: Schematic of the domain for premixed combustion (PC) and partially premixed combustion (PPC) cases.

Due to flame/turbulence interaction the flame front is highly wrinkled. $Z_H$ varies in a wide range from 0.55 to 1.3, whereas $Z_c$ varies in a much narrower range around its value at the initial mixture. This is clearly an effect of the high diffusivity of H2 and relatively low diffusivity of CO, which tends to diffuse more H2 from the preheat zone to the reaction zone, leading to a lower element mass fraction of H in the preheat zone and higher element mass fraction of H in the reaction zone than its value at the unburned mixture.

The effect of differential diffusion on the mixing process and temperature field can be clearly identified in the $Z_H$ and temperature field. At the convex part of the flame front protruding to the unburned mixture $Z_H$ is increased owing to diffusion of H2 from the surrounding unburned fuel/air mixture, which leads to lower $Z_H$ at the concave part of the flame front. The temperature of Syngas flame at the convex part of the flame front is not significantly higher than the concave part of the front. This is likely due to the CO oxidation that compensates partly the loss of H2. At the post flame zone, mixing of the combustion products smooths the gradient of $Z_H$, leading to a decrease of $Z_H$ as compared to its value at the convex part of the flame front. Completion of CO oxidation leads to further increase of temperature in the post-flame zone. This leads to the Z-shaped distribution of the physical cells in the $T$-$Z_H$ diagram. An error arises in the MZCM approach during the mapping of the physical cells to phase space. This error, referred to as *aliasing error* hereafter, is caused during the computation of the mean thermodynamic quantities, e.g., $Y_k$ and $T$, in the phase space. Let $\psi(i,j,j,t_n)$ be a general variable, e.g., $Y_k$ *or* $T$, in cell $(i,j,j)$ at time $t_n$ of the physical domain and $\psi_{MZ}(l,m,t_n)$ be the mean $\psi$ in the corresponding zone $(m,l)$ in the phase space, the aliasing error in the mapping procedure, $\varepsilon_\psi$ , can be defined as

$$\varepsilon_{\psi_{t_n}} = \sqrt{\frac{1}{N_{PC}}\sum\left(\psi(i,j,k,t_n) - \psi_{MZ}\left(i_T(i,j,k,t_n), i_Z(i,j,k,t_n)\right)\right)^2} \tag{12}$$

The aliasing error quantifies the difference between the thermodynamic variables in the phase space and the corresponding ones in the physical domain. If the error constantly approaches to zero when the number of zones increases, the results of full DNS and DNS-MZCM become identical.

Figure 4 shows the aliasing errors of $Y_{H2O}$ at various $N_T$ and $N_Z$; H2O s a typical major species in the flame that can reflect the trend of aliasing errors as the grid in the phase space is refined (the same trend is seen for other species). If the aliasing error decreases to zero when the zones in the phase space are increased, the mapping satisfies the consistency requirement. It is seen that if $Z_E$ is defined based on H atom, $Z_E$=$Z_H$, increasing $N_T$ and $N_Z$ the error rapidly approaches to zero. However, it is not the case when $Z_E$ is defined based on C or O atom.

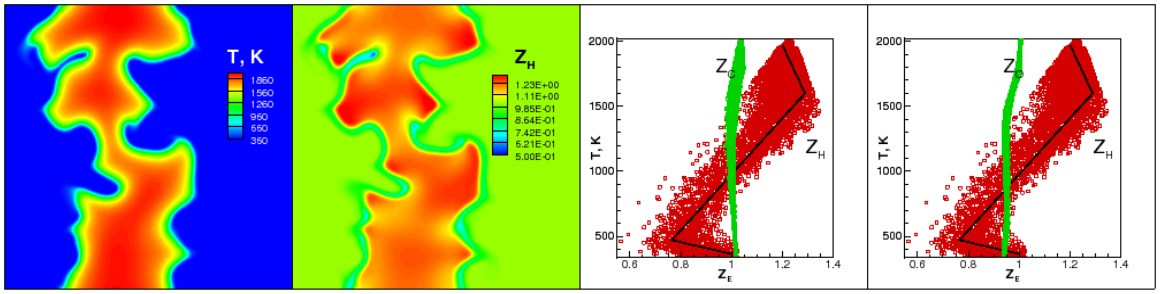


**Figure 3.** PC case; Snapshot of $T$ and $Z_H$ and scatter plot of the physical cells in the $T-Z_E$.

Especially for $Z_E$=$Z_O$ the error appears not to respond to the increasing of $N_T$ and $N_Z$ after an initial decrease, e.g., $N_T$ > 1000 and $N_Z$> 1000. As it was shown in Figure 3, $Z_C$ is a narrow nearly vertical line in the phase space, which implies merging of many physical cells with different thermodynamic states into the same $Z_C$, and as a result $Z_C$ can not discern the different thermodynamic states. This is even worse when $Z_E$=$Z_O$, where variation of $Z_O$ in the horizontal direction is even smaller than that of $Z_C$. The more physical cells are scattered in the phase space in $Z_E$ direction the less is the possibility of merging the information during the mapping them from physical domain to the phase space, thus, the smaller is the error of MZCM. Note that $Z_E$ is an elemental quantity and therefore its variation is only due to differential diffusivity of the species in a premixed mixture. It is evident that to minimize the aliasing error, $Z_E$ should be based on an element which maximizes the variation of $Z_E$ in the phase space. This means the element should be such that it appears in the major species with the maximum differences in their mass diffusivity, e.g, H element for fuel containing H atom.

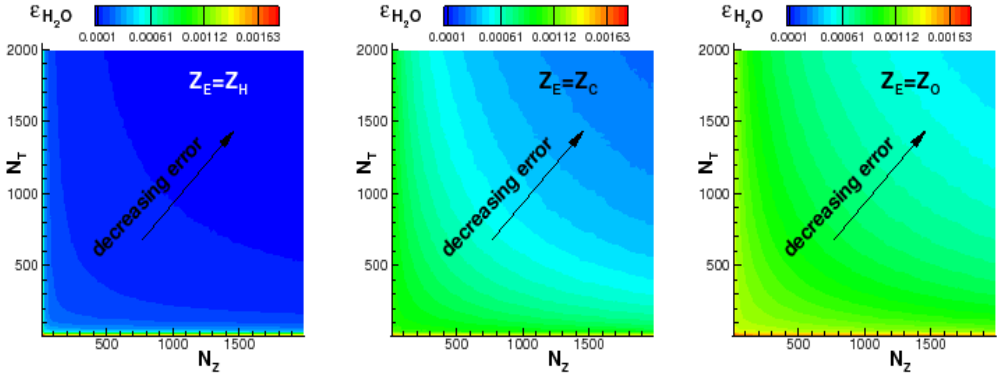


**Figure 4.** Response of aliasing error in $Y_{H2O}$, to the increasing number of zones for premixed H2/CO/N2-air flame.

Figure 5a shows a snapshot of heat-release rate. Figures 5b, 5c and 5d show the results of DNS-MZCM with $N_T$ of 2000, 1000 and 500, respectively, and based on $Z_E$=$Z_H$. $N_Z$ was kept to 1000 in these calculations. With these resolutions in the phase space, the level of the heat release rate and its dependence on the flame front curvature are well simulated. It appears that $N_T$ of 500 is enough for the MZCM simulations of the present Syngas flame.

If the physical space is mapped to $T$-$Z_C$ space in DNS-MZCM the wrinkling structures are seen to be reasonably well simulated, Fig.5e. However, since the variation of $Z_C$ is small in the present flame, as shown in Fig.3, it is not possible to discern the effect of differential diffusion, this leads to that $Z_C$ becomes a unique function of $T$. Mapping to T-$Z_C$ space is equivalent to mapping to T only. As a result the level of heat release rate is independent of the curvature of the reaction front, Fig.5e. Although in the simulation $N_T$= *2000,* which is much larger than that in Fig.5d with a $N_T$= *500,* it does not help to improve the result. This is consistent with the results shown in Fig. 4, and discussion therein regarding the aliasing error when $Z_E$=$Z_C$.

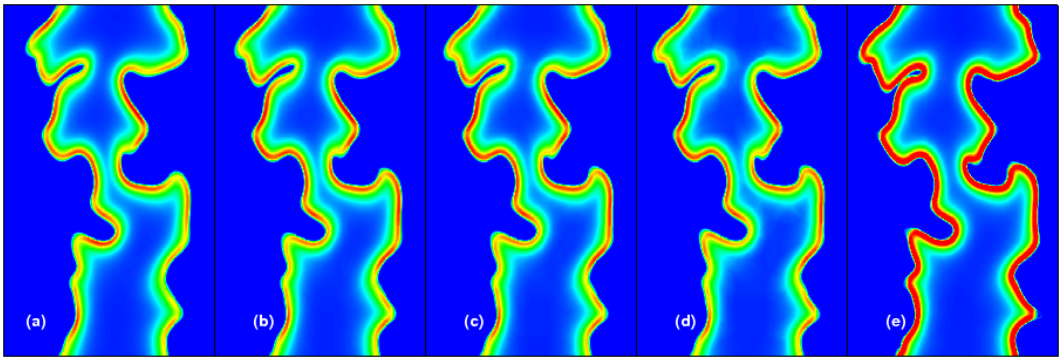


**Figure 5**. Snap-shots of heat release rate and scatter plot of the physical cells in the $T$-$Z_E$ space. Results are from DNS and DNS-MZCM for the premixed turbulent methane/air flame (case PC): (a) DNS; (b) DNS-MZCM with $N_T$=2000; (c) DNS-MZCM with $N_T$=1000; (d) DNS-MZCM with $N_T$=500. (e) DNS-MZCM with $N_T$=2000 and $Z_E$=$Z_C$; in all DNS-MZCM $N_Z$ was set to be 1000. Except (e) in which $Z_E$=$Z_C$, for (b), (c) and (d) $Z_E$=$Z_H$.

## MZCM approach for partially premixed combustion

The MZCM approach is applied to compute a partially premixed combustion (PPC) case. The outline of the initial conditions and the computational domain can be found in Table 1 and schematic in Fig.2. The fuel (syngas) and air are initially non-premixed. The air is at 1100 K while fuel is initially 600 K. First, the fuel and air undergo mixing and as well as rather slow ignition reactions, as the initial temperature of the fuel and air is relatively low. Since the flow in the initial field is turbulence with a Reynolds number of 150, after a short mixing time (<0.3 ms), the composition and temperature fields that were initially perfectly non-premixed are turned to a partially premixed field with both fuel-lean and rich regions.

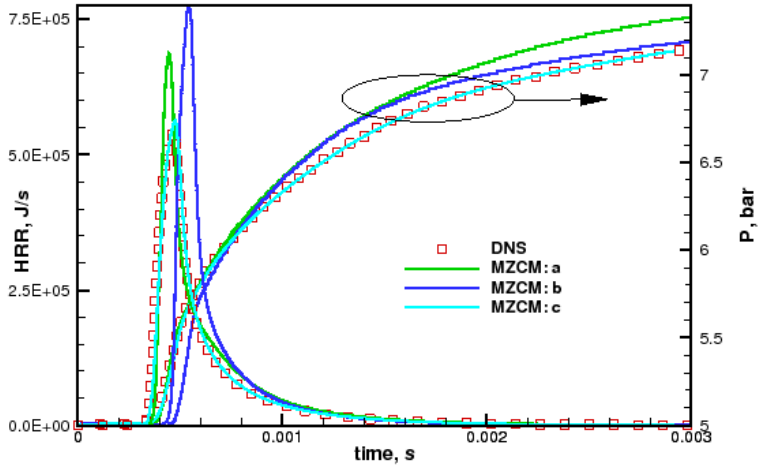


**Figure 6**. History of total heat release rate and mean pressure of the enclosure; MZCM:a is with $Z_E$=$Z_H$; MZCM:b is with $Z_E$=$Z_C$; MZCM:c is with a 3D-phase space of $T$-$Z_H$-$(\nabla Z_H)^2$ ; for all MZCM cases $N_T$=1000 and $N_Z$=*1000*; In MZCM:c; number of zone for $(\nabla Z_H)^2$ is 100.

Figure 6 shows the time history of heat release rate and the mean thermodynamic pressure of the enclosure. Significant heat release rate is seen to start after about 0.3 ms from the start of simulation. The combustion is then continuing as premixed flame propagation. This case mimics the combustion in the partially premixed combustion chambers such as that of a direct injection compression ignition engines.

Mixing quality of a mixture may quantify by elemental equivalence ratio as

$$\varphi = \left(\frac{Y_H + Y_C}{Y_O + Y_N}\right) \Big/ \left(\frac{Y_H + Y_C}{Y_O + Y_N}\right)_{st}. \qquad (13)$$

The subscript *st* is referred to the stoichiometric mixture. $Y_H$, $Y_C$, $Y_O$ and $Y_N$ are the element mass fraction of H, C, O and N atom defined in the Eq.(5). In a premixed combustion the variation of $Y_H$, $Y_C$, $Y_O$ and $Y_N$ are only caused by differential diffusivity of the species (previous PC case); however, the variation of $Y_H$, $Y_C$, $Y_O$ and $Y_N$ in the PPC case is not only because of differential diffusivity of the species but also due to the initial state of the mixture and turbulent mixing.

Figure 7 shows time evolution of the reaction front, the heat release rate and the mixing field in various instances. The first row shows variation of the elemental equivalence ratio (based on Eq. 13). This shows how the turbulence mixing and diffusion develop to a partially premixed mixture with fuel-lean and fuel-rich regions. Combustion in this system involves a coexistence of lean and rich premixed flames as well as non-premixed flames. Using the flame index introduced by Yamashida et. al. [18] the premixed fuel-lean, fuel-rich and non-premixed flames can be identified. For a premixed case, flame index $\xi = \nabla Y_F \cdot \nabla Y_{Ox} > 0$ and for a non-premixed case $\xi = \nabla Y_F \cdot \nabla Y_{Ox} < 0$. The second row of Fig. 7 shows the modified flame index $\xi = (\nabla Y_{H2} + \nabla Y_{CO}) \cdot \nabla Y_{O2}$. In the region marked by a circle, for example, the flame is a non-premixed one. However, in the region pointed by an arrow a lean and a rich premixed flame meet a non-premixed flame to form a triple point.

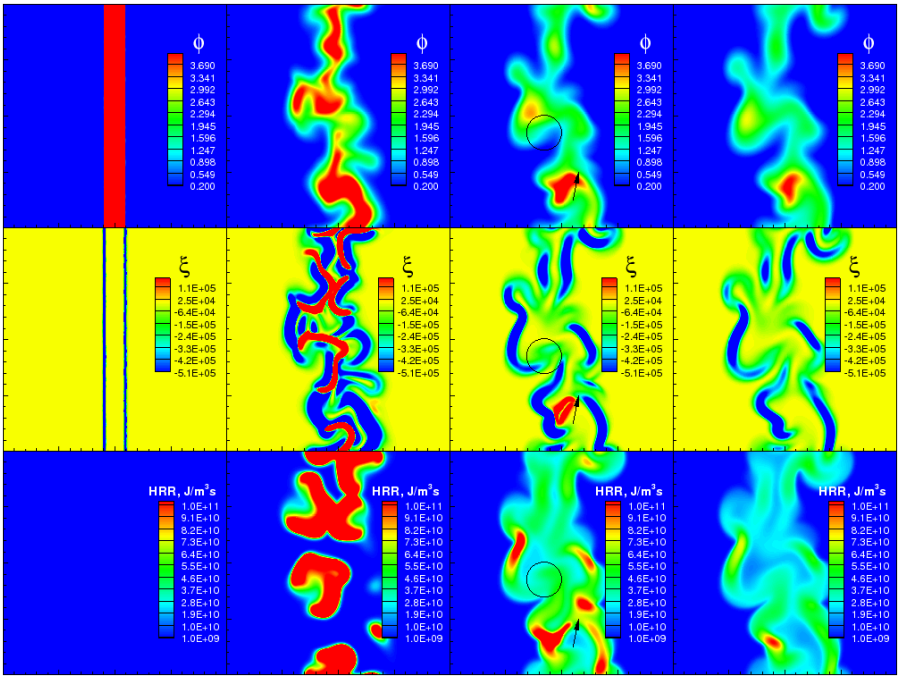


**Figure 7.** DNS results for the PPC case; Snap-shots of elemental equivalence ratio Φ (first row), flame index ξ (second row) and heat release rate (third row); from left to right: 0, 0.425, 0.532 and 0.580 ms after the start of simulation, respectively.

Figure 8 shows the performance of MZCM in the simulation of partially premixed combustion. Fig.8a shows DNS results. Figs.8b-d show the results of DNS-MZCM. The phase-space in Fig.8b is $T$-$Z_H$ while in Fig.8c the phase-space is $T$-$Z_C$. It is evident that neither of these two phase spaces can adequately simulate the process. The previously successful $T$-$Z_H$ mapping for the premixed flames is not suitable for the PPC case.

For the PC cases the key process to be taken into account in the mapping of the physical cells to the phase-space is species differential diffusion, which results in variation in $Z_E$. However, in a partially premixed combustion, variation of $Z_E$ is not only a consequence of mass diffusion but also caused by the initial state and turbulent mixing. As such, it is

reasonable to add a third dimension to the $T$-$Z_E$ phase-space in order to address the variation of $Z_E$ due to turbulent mixing of the initially non-premixed fuel and air.

We propose to use $\xi = \nabla Z_H \cdot \nabla Z_H$ as the third phase space variable. $\xi$ is proportional to the scalar dissipation rate of $Z_H$ and hence, variation of $Z_H$ due to turbulent mixing. Fig.8d shows the results of DNS-MZCM with a 3D phase-space of $T$-$Z_H$- $\nabla Z_H \cdot \nabla Z_H$. It is evident that by adding the third dimension $\nabla Z_H \cdot \nabla Z_H$ and mapping physical cells to this 3D phase space of $T$-$Z_H$- $\nabla Z_H \cdot \nabla Z_H$ significant enhancement of the performance of DNS-MZCM is achieved in the computing of the PPC case.

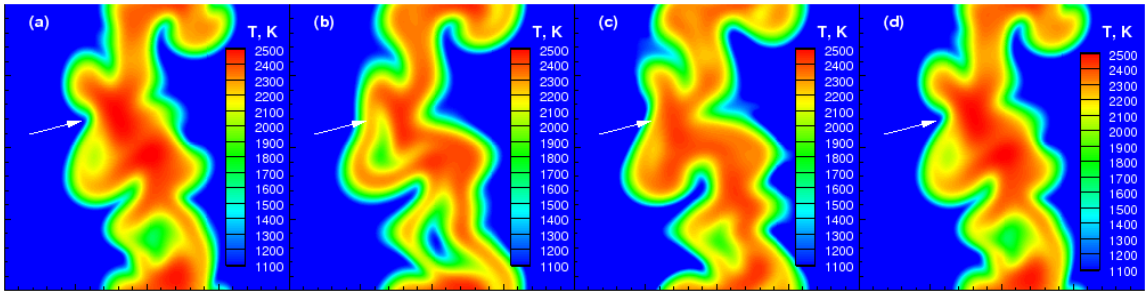


**Figure 8.** Snap-shots of temperature for the PPC case 0.602 ms after the start of simulation; (a) DNS; (b) DNS-MZCM with $Z_E$=$Z_H$; (c) DNS-MZCM with $Z_E$=$Z_C$; (d) DNS-MZCM with a 3D-phase space of $T$-$Z_H$- $\nabla Z_H \cdot \nabla Z_H$ ; for all cases $N_T$=1000 and $N_Z$=*1000*; In (d) number of 100 zones for $\nabla Z_H \cdot \nabla Z_H$ .

Finally, we note that the same conclusion can be drawn from Fig.6 where the global heat release rate and the thermodynamic pressure from the DNS-MZCM with the three dimensional phase space are almost identical to the DNS results, whereas mappings based on $T$-$Z_H$ are not sufficient.

## Conclusions

An efficient multi-zone chemistry mapping (MZCM) approach is developed to couple detailed chemical kinetics to direct numerical simulation (DNS) of the combustion processes in premixed and partially premixed fuel/air mixtures in constant volume enclosures. Different phase spaces for MZCM and the aliasing errors from the mapping procedure are investigated. Based on the DNS and DNS-MZCM results the following conclusions are drawn.

(a) From the DNS results it is found that after the ignition the element mass fractions in the initially premixed fuel/air mixture become non-uniform in the physical space. This is due to differential diffusion in the species. Based on this observation, we introduce a specific mass ratio of element $Z_E$ at a given location in the physical domain, which is the ratio of the mass fraction of element $E$ at the location to its corresponding value at the unburned stoichiometric mixture. The specific mass ratio of the element that is involved in the most diffusive molecules, e.g. H-atom in fuels involving H-atoms, is most suitable to define the phase space together with the temperature for the multi-zone chemistry mapping.

(b) For element that is involved in species with Lewis number close to the unity, e.g. O-atom or C-atom, the scatter of the physical cells in the phase space is very narrow with rather small variation in its maximum and minimum element mass ratios at a given temperature. This implies that the specific element mass ratio based on these elements cannot discern the different mixing states and the thermodynamic states during combustion. If the phase space is defined based on these elements, the aliasing errors introduced in the mapping procedure can be very high. In general the errors do not approach to zero when the resolution in the phase space is refined. Important phenomena such as local extinction and the effect of curvature/flame stretch on the radical concentration and the heat release rate at the reaction zones cannot be captured with such phase space.

(c) It was found in a partially premixed combustion where the variation of $Z_E$ is a function of both differential diffusivity and turbulent mixing of the initially non-premixed state, adding a third dimension to the $T$-$Z_E$ is required. This third parameter should identify turbulent mixing in the physical cells. An modified scalar dissipation rate of $Z_E$ in the physical cells, $\nabla Z_H \cdot \nabla Z_H$, was shown to be suitable for this purpose, and it was shown the results of DNS and DNS-MZCM with a 3D phase-space $T$-$Z_H$- $\nabla Z_H \cdot \nabla Z_H$ are identical.

**Acknowledgments**
This work was sponsored by the Swedish Research Council (VR), the Competence Centre for Combustion Process at Lund University (KC-FP), and the national Centre for Combustion Science and Technology (CeCOST). The computation was performed using the computer facilities provided by the Centre for Scientific and Technical Computing at Lund University (LUNARC) and the Swedish National Infrastructures for Computing (SNIC).

**References**
[1] Barlow, R. S., Frank, J. H., "Effects of turbulence on species mass fractions in methane/air jet flames," *Proc. Comb. Inst.*, 27: 1087-1095 (1998).
[2] Vreman, A. W., Albrecht, B. A., van Oijen, J. A., de Goey, L. P. H., Bastiaans, R. J. M., "Premixed and nonpremixed generated manifolds in large-eddy simulation of Sandia flame D and F," *Comb. Flame,* 153:394-416 (2008).
[3] Bilger, R. W., Pope, S. B., Bray, K. N. C., Driscoll, J. F., "Paradigms in turbulent combustion research," *Proc. Comb. Inst.,* 30:21-42 (2005).
[4] Hilbert, R., Tap, F., El-Rabii, H., Thévenin, D., "Impact of detailed chemistry and transport models on turbulent combustion simulations", *Prog. Ener. Comb.*30:61-117 (2004).
[5] Lam, S. H., Coussis, D. A., "Understanding complex chemical kinetics with computational singular perturbation," *Proc. Comb. Inst.,* 22:931-941 (1989).
[6] Mass, U., Pope, S. B., "Laminar flame calculations using simplified chemical kinetics based on intrinsic low-dimensional manifolds", *Proc. Comb. Inst.,* 25:1349-1356 (1994).
[7] Jangi, M., Yu, R., Bai, X.S., "A multi-zone chemistry mapping approach for DNS of auto-ignition and flame propagation in a constant volume enclosure", *Comb. Flame,* submitted.
[8] Aceves, M. S., Flowers, D.L., Martinez-Frias, J., Smith, J.R., Westbrook, C.K., Pitz, W., Dibble, R., Christensen, M., Johansson, B., "A multi-zone model for prediction of HCCI combustion and emissions", *Paper No. SAE 2000-01-0327* (2000).
[9] Careta, A., Sagues, F., Sancho, J. M., "Stochastic Generation of Homogeneous Isotropic Turbulence with Well-Defined Spectra," *Phy. Rev. E,* 48:2279-2287 (1993).
[10] Pope, S. B., *Turbulent flows*. Cambridge, UK ; New York: Cambridge U. Press, 2000.
[11] Yetter, R. A., Dryer, F.L., Rabitz, H., "A Comprehensive Reaction Mechanism For Carbon Monoxide/Hydrogen/Oxygen Kinetics", *Combust. Sci. Tech.,* 79:97-128 (1991).
[12] Day, M. S., Bell, J.B. , "Numerical Simulation of Laminar Reacting Flows with Complex Chemistry," *Combust. Theory Modelling,* 4:535-556 (2000).
[13] Shi, J., Hu, C. Q., Shu, C. W., "A technique of treating negative weights in WENO schemes," *J. Compu. Phy.,* 175:108-127 (2002).
[14] Gottlieb, S., Shu, C. W., "Total variation diminishing Runge-Kutta schemes", *Math. Compu.*, 67:73-85 (1998).
[15] R. Yu, "Large Eddy Simulation of Turbulent Flow and Combustion in HCCI engines", Doctoral Thesis, Lund university, 2008.
[16] Lutz, A. E., Kee, R.J., Miller, J.A., "SENKIN: A FORTRAN program for predicting homogeneous gas phase chemical kinetics with sensitivity analysis", SAND87-8248 (1997) .
[17] Barths, H., Felsch, C., Peters, N., "Mixing models for the two-way-coupling of CFD codes and zero-dimensional multi-zone codes to model HCCI combustion", *Comb. Flame*, 156:130–139 (2009).
[18] Yamashita, H., Shimada, M., Takeno, T., "A numerical study on flame stability at the transition point of jet diffusion flames", Proc. Comb. Inst., 26:27-34 (1996).